Distribution, transport, and degradation of apolipoprotein B-100 in HepG2 cells

Nobuhiro Sakata,[1,*] Thomas E. Phillips,[†] and Joseph L. Dixon[2,*]

Dalton Cardiovascular Research Center* and Division of Biological Sciences,† University of Missouri, Research Park, Columbia, MO 65211

Abstract **The transport of apolipoprotein B (apoB) between the endoplasmic reticulum (ER) and Golgi was studied in puromycin-synchronized HepG2 cells, using an antibody that could distinguish between apoB in ER and Golgi compartments. In cells with normal ER-to-Golgi transport, both albumin and apoB colocalized throughout the ER and appeared as intense, compact signals in Golgi. When ER-to-Golgi transport was blocked with brefeldin A, apoB and albumin remained colocalized in the ER network and three-dimensional constructed images showed more intense signals for both proteins in a central, perinuclear region of the ER. When protein synthesis was stopped in cells with brefeldin A-inhibited ER-to-Golgi transport, apoB degradation was visualized as a homogeneous decrease in fluorescence signal intensity throughout the ER that could be slowed with *clasto*-lactacystin β-lactone, a proteasome inhibitor. Incubation of cells with CP-10447, an inhibitor of microsomal triglyceride transfer protein, inhibited apoB, but not albumin, transport from ER to Golgi. Nanogold immunoelectron microscopy of digitonin-permeabilized cells showed proteasomes in close proximity to the cytosolic side of the ER membrane. Thus, newly synthesized apoB is localized throughout the entire ER and degraded homogeneously, most likely by neighboring proteasomes located on the cytosolic side of the ER membrane. Although albumin is colocalized with apoB in the ER, as expected, it was not targeted for ER-associated proteasomal degradation.**—Sakata, N., T. E. Phillips, and J. L. Dixon. **Distribution, transport, and degradation of apolipoprotein B-100 in HepG2 cells.** ***J. Lipid Res.*** **2001.** 42: **1947–1958.**

Supplementary key words albumin • endoplasmic reticulum • Golgi • microsomal triglyceride transfer protein • proteasome • protein degradation • puromycin • three-dimensional imaging

Apolipoprotein B-100 (apoB) is the structural protein for plasma VLDL and LDL and is synthesized primarily in hepatocytes (1, 2). The secretion rate of apoB is an important factor determining the concentrations of apoB lipoproteins and cholesterol in blood (2, 3). The rate of apoB secretion can vary during the course of the day within individuals (4), and has been observed to be increased in patients with hyperlipidemias (5). Studies to decipher the subcellular mechanisms regulating apoB and VLDL secretion have been performed largely in cultured cells. ApoB is synthesized on ribosomes attached to the endoplasmic reticulum (ER) and translocated through the ER membrane, and lipids are added to nascent apoB cotranslationally or posttranslationally [for a comprehensive review see Davis (2)]. ApoB-lipoprotein particles are enlarged in subsequent lipidation steps, either in the ER (6) or in post-ER compartments (7). Microsomal triglyceride transfer protein (MTP) is an ER lumenal protein that carries triglyceride and phospholipid to nascent apoB molecules (8, 9) and participates in early apoB-lipoprotein assembly (10). Additional steps in the assembly of apoB-lipoproteins, especially transport from ER to Golgi, are less well understood. Only small, dense apoB-lipoprotein particles were observed in the ER (10), indicating that bulk transfer of lipids may occur post-ER. By the time apoB is transported to the plasma membrane and secreted into blood, it is part of a VLDL particle that varies between 20 and 70 nm in diameter.

One mechanism that regulates apoB secretion is cotranslational or posttranslational degradation (11–13). ApoB is a substrate for the cytosolic ubiquitin-proteasome system (14–17). Much larger than other proteins that undergo ER-associated degradation (18–21), apoB, located in the ER lumen but associated with the ER membrane (22), requires delipidation, deglycosylation, and retrograde transport before degradation by cytosolic or ER membrane-associated proteasomes (17, 23). An important advance to the translocation arrest model (11, 23, 24) for ER apoB degradation was elucidated with the breakthrough observation that apoB remains engaged to the ribosome and translocon and is not fully translated until nascent lipoprotein assembly progresses sufficiently (25). Therefore, underlipidated apoB can be drawn back through the

Abbreviations: apoB, apolipoprotein B-100; ER, endoplasmic reticulum; MTP, microsomal triglyceride transfer protein.

[1] Present address: Division of Atherosclerosis, Nutrition and Lipid Research, Washington University School of Medicine, St. Louis, MO 63110.

[2] To whom correspondence should be addressed.
e-mail: dixonj@missouri.edu

translocon for degradation by the proteasome, probably with the aid of cytosolic chaperons (26).

There are other pathways of apoB degradation in addition to proteasomal degradation. The kinetics of intracellular apoB degradation are relatively slow in rat hepatocytes, indicating that apoB degradation occurs largely in a post-ER compartment in rodent hepatocytes (27–29). It has been proposed that degradation of apoB may involve interactions with the LDL receptor in the secretory pathway (30).

In the current work, we were able to deplete apoB and albumin from the secretory pathway with puromycin, and apoB transport between ER and Golgi was studied in reinitiated cells, using an antibody that could distinguish between apoB in ER and Golgi. Our results show that apoB and albumin, proteins with vastly different posttranslational modification itineraries, colocalize throughout the extensive ER under normal transport conditions and when ER-to-Golgi transport is inhibited by brefeldin A. In contrast to albumin, which is stable in the secretory pathway, apoB was degraded homogeneously in the ER when ER-to-Golgi transport was blocked with brefeldin A. These observations are consistent with the colocalization of apoB and the proteasome throughout the extensive ER network (17).

MATERIALS AND METHODS

Materials

Anti-proteasome β-type subunits, HC10 and LMP7, were purchased from Affiniti (Mamhead, UK). Anti-Golgin-97 was obtained from Molecular Probes (Eugene, OR). The C1.4 and CC3.4 monoclonal antibodies to apoB were gifts of G. Schonfeld (Washington University, St. Louis, MO). Rabbit anti-human albumin (no. 55110) was purchased from Organon Teknika (Cappel) (Durham, NC). Secondary antibodies conjugated with fluorochromes (Cy3 or Cy5) were obtained from Jackson ImmunoResearch Laboratories (West Grove, PA). Puromycin and brefeldin A were purchased from Sigma (St. Louis, MO). An MTP inhibitor, CP-10447, was provided by Pfizer (Groton, CT) (31). *clasto*-Lactacystin β-lactone was obtained from Novabiochem. MEM and cell culture reagents were purchased from Life Technologies (Grand Island, NY). All other chemicals were of the highest purity available.

Cell culture

HepG2 cells were grown in MEM with 0.1 mM nonessential amino acids, 1 mM sodium pyruvate, penicillin (100 U/ml), streptomycin (100 μg/ml), and 10% fetal bovine serum on collagen-coated cover slips as previously described (22). Cells that were 20–30% confluent were used for immunocytochemistry experiments.

Depletion and replenishment of apoB and albumin in HepG2 cells

In all experiments, HepG2 cells were first preincubated with serum-free medium (containing 1.5% BSA but without fatty acid supplement) for 60 min at 37°C. To deplete cellular apoB and albumin, cells were incubated with medium containing puromycin (20 μM) for 120 min at 37°C. To reinitiate protein synthesis, cells were washed with warmed PBS three times and incubated with serum-free medium (containing 1.5% BSA) without puromycin for up to 60 min at 37°C and analyzed by immunocytochemistry, using anti-apoB and anti-albumin antibodies.

Inhibition of protein transport

Brefeldin A (2 μg/ml) was used to interrupt protein transport between the ER and Golgi. MTP inhibitor CP-10447 (20 μM) was used to inhibit lipidation of apoB. In some experiments cells were washed with cold PBS three times and incubated with cold serum-free medium with or without inhibitors (brefeldin A or CP-10447) at 4°C for 30 min to prevent reinitiation of protein synthesis and transport, and to allow access of the inhibitors to their sites of action. After incubation, cells were washed with warmed PBS and incubated at 37°C for 60 min with serum-free medium with or without inhibitors.

Degradation of newly synthesized apoB

To study sites of apoB degradation, transport of newly synthesized apoB and albumin was inhibited by brefeldin A. After 120 min of incubation with brefeldin A, puromycin (20 μM) was added to medium with brefeldin A to inhibit replenishment of the apoB pool in ER by protein synthesis.

Cell permeabilization and immunocytochemistry

Cell fixation and permeabilization procedures were described previously (17, 22). Saponin was used to perforate both plasma and intracellular membranes, and digitonin was used to perforate only the plasma membrane. For permeabilization of cells with saponin for immunocytochemistry, cells were washed twice with PBS, fixed in 2% paraformaldehyde for 30 min, washed three times with intracellular buffer (75 mM potassium acetate, 2.5 mM magnesium acetate, 1.8 mM calcium chloride, 25 mM HEPES buffer, pH 7.2), and permeabilized with 0.1% saponin in intracellular buffer with 0.1% BSA for 30 min at room temperature. All subsequent steps for saponin-permeabilized cells were performed in intracellular buffer containing 0.1% saponin and 0.1% BSA. For permeabilization of cells with digitonin for immunocytochemistry, HepG2 cells were washed twice with PBS (4°C) and treated for 5 min at 4°C with digitonin (60 μg/ml) in intracellular buffer. After removing digitonin, the cells were washed three times with intracellular buffer and then fixed with 2% paraformaldehyde for 30 min at room temperature and processed for immunocytochemistry. Saponin- or digitonin-permeabilized cells were incubated overnight with primary antibodies and then incubated for 4 h with the appropriate anti-mouse or anti-rabbit IgG secondary antibodies conjugated with fluorochromes (Cy3 or Cy5). The coverslips were mounted on glass slides with Mowiol and examined with an MRC-600 confocal microscope (Bio-Rad, Hercules, CA) as described in detail by Du et al. (22).

Extremely low fluorescence ("background") was observed when permeabilized cells were treated with preimmune serum and secondary antibodies, or primary antibodies without secondary antibodies. Confirmation of the specificity of the primary antibodies was obtained when we were able to diminish their signals by treating cells with puromycin and allowing apoB or albumin to be degraded or secreted (see Fig. 2).

Analysis of immunocytochemistry data

ApoB, albumin, and proteasome signals from immunocytochemistry were analyzed with the NIH Image program (version 1.62), on a Power Macintosh G3 system (Apple Computer). Three-dimensional images were constructed with Metamorph (version 4.0) on a Dell computer. Mean pixel intensities for cytosolic apoB and albumin signals were measured using NIH Image. Signal intensity and area of an entire cell were measured and sig-

nals in the nucleus were subtracted from total cellular signals. Mean pixel intensity in each cell was calculated by dividing the total nonnuclear signal intensity by total nonnuclear pixel number. Mean pixel intensities between treatment groups were compared.

Nanogold immunoelectron microscopy

After fixation in cold PF fixative (2% freshly depolymerized paraformaldehyde, 70 mM NaCl, 30 mM HEPES, 2 mM $CaCl_2$, pH 7.4) for 1 h, cells were permeabilized with digitonin (60 μg/ml) for 5 min at 4°C, rinsed, and refixed for 1 h. After washing in HEPES wash buffer (HWB: 70 mM NaCl, 30 mM HEPES, pH 7.4), reactive aldehyde groups were blocked by incubation in 50 mM glycine in HWB for 15 min. Nonspecific binding was blocked with 1% normal goat serum, 0.8% BSA, 0.2% ovalbumin, and 0.1% Micr-O-protect (Boehringer Mannheim, Indianapolis, IN) in HWB for 4 h. Cells were then incubated overnight with primary antibodies that had been diluted in HWB. After extensive rinsing, the cells were incubated in a 1:50 dilution of 1-nm gold-conjugated goat anti-rabbit or anti-mouse IgG for 1 to 24 h. Silver enhancement was performed with an HQ kit (Nanoprobes, Stony Brook, NY) for 4 to 8 min according to the manufacturer's protocol. Cells were postfixed in 0.1% osmium tetroxide for 15 min, stained en bloc with 1% uranyl acetate for 1 h, dehydrated with an ethanol series, and embedded in EmBed 812 epoxy resin (Electron Microscopy Sciences, Fort Washington, PA).

Statistical analysis

Unpaired Student's *t*-tests were used to compare results obtained in experiments for degradation of apoB and albumin. A value of $P < 0.05$ was considered significant.

RESULTS

Localization of apoB and albumin in HepG2 cells at steady state

Saponin permeabilization perforates plasma and intracellular membranes and can be used to detect intracellular apoB in the secretory pathway of HepG2 cells (22). Saponin-permeabilized HepG2 cells (**Fig. 1**) were probed with monoclonal anti-human apoB (C1.4)/anti-mouse IgG-Cy3 (Fig. 1A) and rabbit anti-human albumin/anti-rabbit IgG-Cy5 (Fig. 1B) to identify the intracellular locations of these proteins. Albumin signals were seen throughout the ER and were highly concentrated in a focal juxtanuclear region (Fig. 1B) that was confirmed as Golgi, as it colocalized with signals from an antibody to a Golgi marker protein, Golgin-97 (Fig. 1C–E). ApoB signals (probed with the C1.4 monoclonal anti-apoB antibody; Fig. 1A) were also detected throughout the ER, with stronger staining observed in the juxtanuclear region that overlapped with intense albumin staining. We have previously shown that apoB, when probed with a series of other monoclonal and polyclonal antibodies, colocalizes with p63, a resident ER protein (22). The strong staining for apoB that overlaps with strong albumin and Golgin-97 staining shows that the C1.4 antibody provides distinctive staining for apoB in the Golgi. Because C1.4 anti-apoB and anti-Golgin-97 are both monoclonal

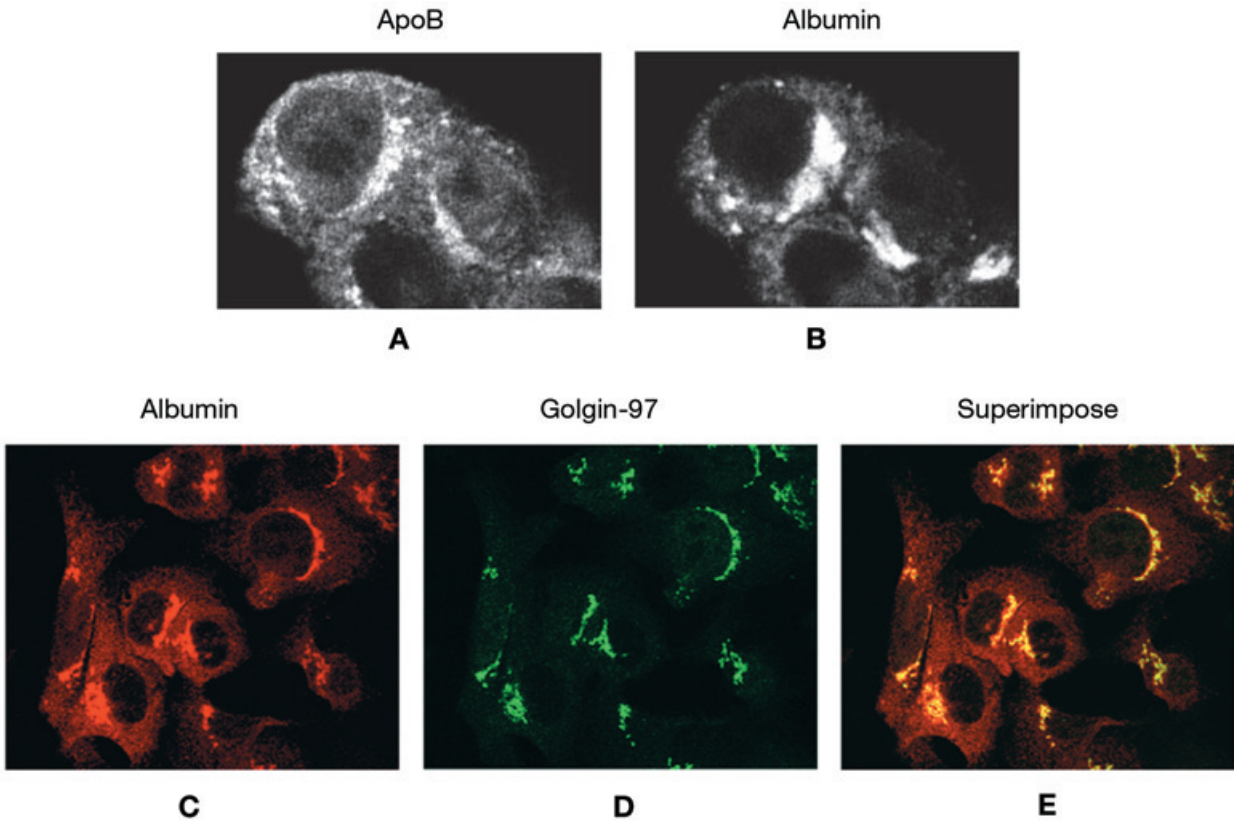

Fig. 1. Localization of apoB and albumin in HepG2 cells. HepG2 cells grown for 2 days on coverslips, were incubated for 1 h in serum-free medium without fatty acid, fixed in 2% paraformaldehyde, and permeabilized with 0.1% saponin to expose all internal compartments to the antibodies. Permeabilized cells were probed simultaneously with mouse anti-apoB antibody C1.4 (A, 1:200 dilution) and rabbit anti-albumin (B, 1:2,500 final dilution), followed by anti-mouse and anti-rabbit IgG secondary antibodies (1:100 dilution) conjugated with fluorochromes (Cy3 or Cy5). In (C–E), cells were probed with rabbit anti-albumin (C) and mouse anti-Golgin-97 (D); (E) shows the signals superimposed.

antibodies, we took advantage that intense, focal, albumin labeling consistently colocalized with Golgin-97 staining and used the intense albumin labeling as a surrogate marker for Golgi in later transport studies.

ApoB depletion and replenishment assay

An apoB depletion and replenishment assay was used to observe newly synthesized apoB transport in single HepG2 cells. Puromycin was used to deplete the majority of apoB and albumin from cells (see protocol in **Fig. 2A**). After 120 min of incubation in medium containing 20 μM puromycin, signals for both apoB and albumin were decreased considerably, indicating that a large proportion of apoB and albumin had been lost from the cells, because of secretion or degradation [Fig. 2B, compare panels b and g (0 min of reinitiation) with panels a and f (control cells without puromycin treatment)]. Reinitiation of apoB and albumin synthesis occurred when puromycin-containing medium was removed and cells were incubated in serum-free medium at 37°C. Signals for apoB and albumin were still diminished after 5 min of reinitiation (Fig. 2B, panels c and h), but could be seen throughout the ER with strong staining in the focal juxtanuclear region at 30 min (Fig. 2B, panels d and i), indicating transport to the Golgi had already occurred. The observations with albumin agree with those of Mizuno and Singer (32), who observed significant transfer of albumin to Golgi in HepG2 cells 21 min after cycloheximide washout. The current data with apoB indicate that apoB transfer to the Golgi is also rapid. At 60 min after reinitiation (Fig. 2B, panels e and j), the patterns of signals for cellular apoB and albumin were similar to those seen in control cells that had not been treated with puromycin. These data indicate that 2 h of puromycin treatment is sufficient to largely deplete cells of apoB and albumin, and reinitiation of apoB and albumin synthesis and interorganelle transport occur rapidly and efficiently after washout of puromycin.

Effects of inhibition of ER-to-Golgi transport on apoB and albumin distribution in the ER

The rapid transfer of apoB and albumin from ER to Golgi after reinitiation of protein synthesis prevented use of this protocol alone to study the distribution of apoB and albumin in the ER. For this reason, we included a "transport inhibition" step in which cells were incubated with brefeldin A for 30 min at 4°C immediately after removal of puromycin to inhibit ER-to-Golgi transport before reinitiation of protein synthesis (see protocol in **Fig. 3A**). This step did not slow subsequent reinitiation of protein synthesis. With ER-to-Golgi transport blocked, similar distributions for apoB and albumin were observed in the extensive ER network after 60 min of renewed protein synthesis (Fig. 3B, panels b and e).

We wished to test whether inhibition of apoB-lipoprotein assembly would alter apoB transport and distribution. One potential step to block is MTP, a protein that shuttles triglyceride and phospholipid from ER membranes to apoB in the ER lumen (8, 9). Treatment of apoB- and albumin-depleted cells with CP-10447, an inhibitor of MTP (31), prevented apoB from reaching the focal juxtanuclear Golgi region in the period after reinitiation of protein synthesis (Fig. 3B, panel c). ApoB was localized throughout the ER, showing a pattern similar to that of apoB in cells that were treated with brefeldin A. Albumin synthesis and transport were minimally affected by CP-10447 (Fig. 3B, panel f), indicating that apoB transport from ER to

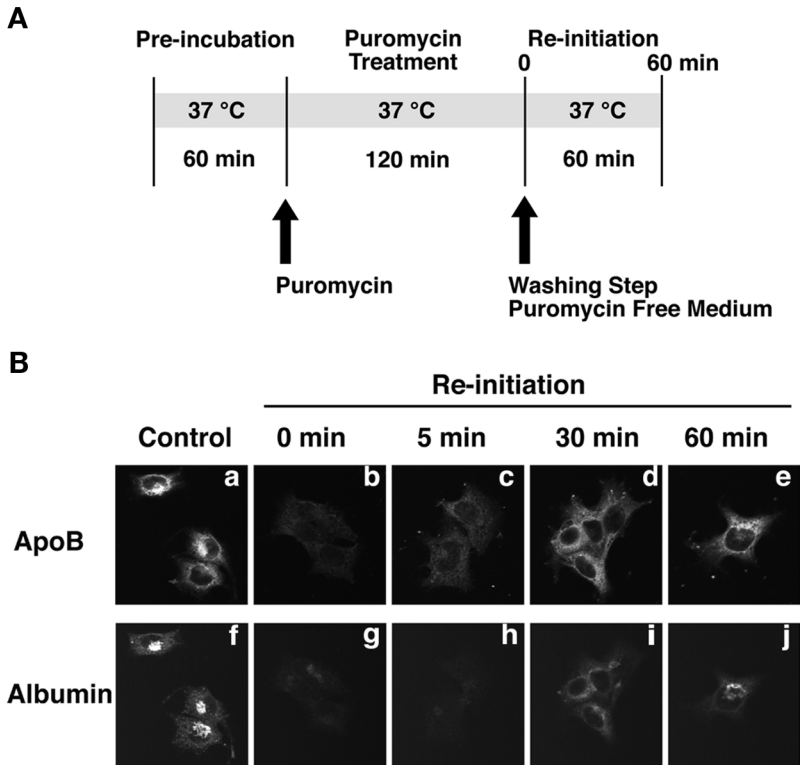

Fig. 2. Depletion and replenishment of apoB and albumin in HepG2 cells. A: Experimental protocol: after preincubation with serum-free medium for 1 h, cells were incubated in medium plus puromycin (20 μM) for 120 min to deplete intracellular apoB and albumin. Reinitiation of apoB and albumin synthesis and transport occurred after puromycin-containing medium was removed and cells were incubated in fresh serum-free medium for up to 60 min. B: At each time point, cells were fixed, permeabilized, and probed with mouse anti-apoB (C1.4, 1:100 dilution) and rabbit anti-albumin (1:2,500 dilution) antibodies followed by the appropriate secondary antibodies. Control denotes cells harvested before puromycin treatment (a and f). a–e: ApoB signals; f–j: albumin signals.

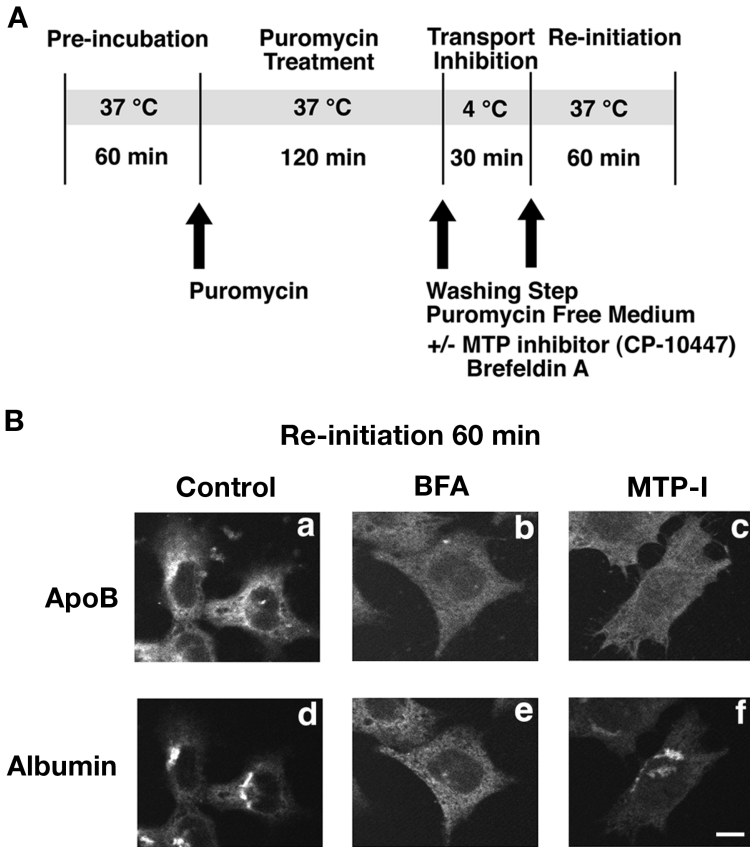

Fig. 3. Inhibition of apoB transport with brefeldin A and CP-10447, an MTP inhibitor. A: Experimental protocol: after preincubation with serum-free medium, cells were cultured in medium with puromycin (20 μM) for 120 min at 37°C to deplete apoB and albumin. Cells were washed and incubated at 4°C for 30 min without puromycin in the presence of brefeldin A (BFA, 2 μg/ml; b and e) or CP-10447 (MTP-I, 20 μM; c and f). Protein synthesis was then restarted when the medium was replaced with fresh 37°C medium without puromycin but containing brefeldin A (b and e) or CP-10447 (c and f). B: After 60 min of reinitiation of protein synthesis, cells were fixed, permeabilized, and probed with anti-apoB (C1.4; a–c) and anti-albumin (d–f) followed by the appropriate secondary antibodies. Control (a and d) denotes cells that were treated identically as experimental cells but without inhibitors. Magnification bar: 10 μm.

Golgi was specifically affected when MTP-dependent lipid transfer was interrupted with CP-10447.

Three-dimensional distribution of albumin and apoB in control cells and cells with blocked ER-to-Golgi transport

In previous experiments only signals for apoB and albumin from single horizontal confocal x-y sections of cells were shown. To study the distribution of apoB and albumin more rigorously, it was necessary to probe through multiple x-y sections and determine the three-dimensional distribution of apoB and albumin in the ER and Golgi. Multiple x-y sections through control (without transport inhibition) and brefeldin A-treated cells (with interrupted apoB and albumin transport) were scanned 60 min after reinitiation of protein synthesis. Three-dimensional images were constructed and signal intensity was displayed as pseudocolors (see scale at bottom of **Fig. 4**). In a control cell (Fig. 4A, panel a), the three-dimensional view indicated that albumin was distributed throughout the ER (purple, blue) with a highly concentrated signal (white, red, and yellow) in the Golgi (seen in this cell as two nodes in the focal juxtanuclear region). When the view of the cell was rotated to 0° (view from side) (Fig. 4A, panels b–d), albumin signals were observed at every z level in the ER and, in this particular cell, the Golgi was observed as a compact doublet structure that spanned almost the entire vertical thickness of the cell. When ER-to-Golgi transport was interrupted with brefeldin A (Fig. 4A, panels e–h), signals for albumin were not detected in Golgi but were observed throughout the ER, including regions that were immediately adjacent to the plasma membrane. In the same control cell depicted in Fig. 4A, apoB (Fig. 4B, panels i–l) was also observed throughout the ER (blue), with a concentrated doublet signal (red, yellow) in the Golgi (Fig. 4B, panel l). In brefeldin A-treated cells, apoB was distributed in the ER similar to albumin, and was not seen in the Golgi. Analysis of the three-dimensional images of the brefeldin A-treated cells (providing manyfold more signal than available from a single confocal plane) indicated that there was increased signal intensity for both albumin (Fig. 4A, panels e–g) and apoB (Fig. 4B, panels m–o) in a broad central portion of the ER surrounding the nucleus (seen as yellow). The stronger signals in the central regions were also seen with the 0° view (Fig. 4: albumin, panel h; apoB, panel p). Therefore, in cells with blocked ER-to-Golgi transport, apoB and albumin are synthesized and remain throughout the extensive ER network, including central areas with increased signal intensity and other areas that are immediately adjacent to the plasma membrane.

ApoB degradation in brefeldin A-blocked cells

We reported that apoB degradation was more rapid in brefeldin A-treated HepG2 cells (33) and that apoB and the proteasome colocalize throughout the ER of the cell (17). The latter observation led us to hypothesize that degradation of apoB in the ER should occur widely, and would not require transport to a specific region in the ER or to a separate organelle. To test this hypothesis, we in-

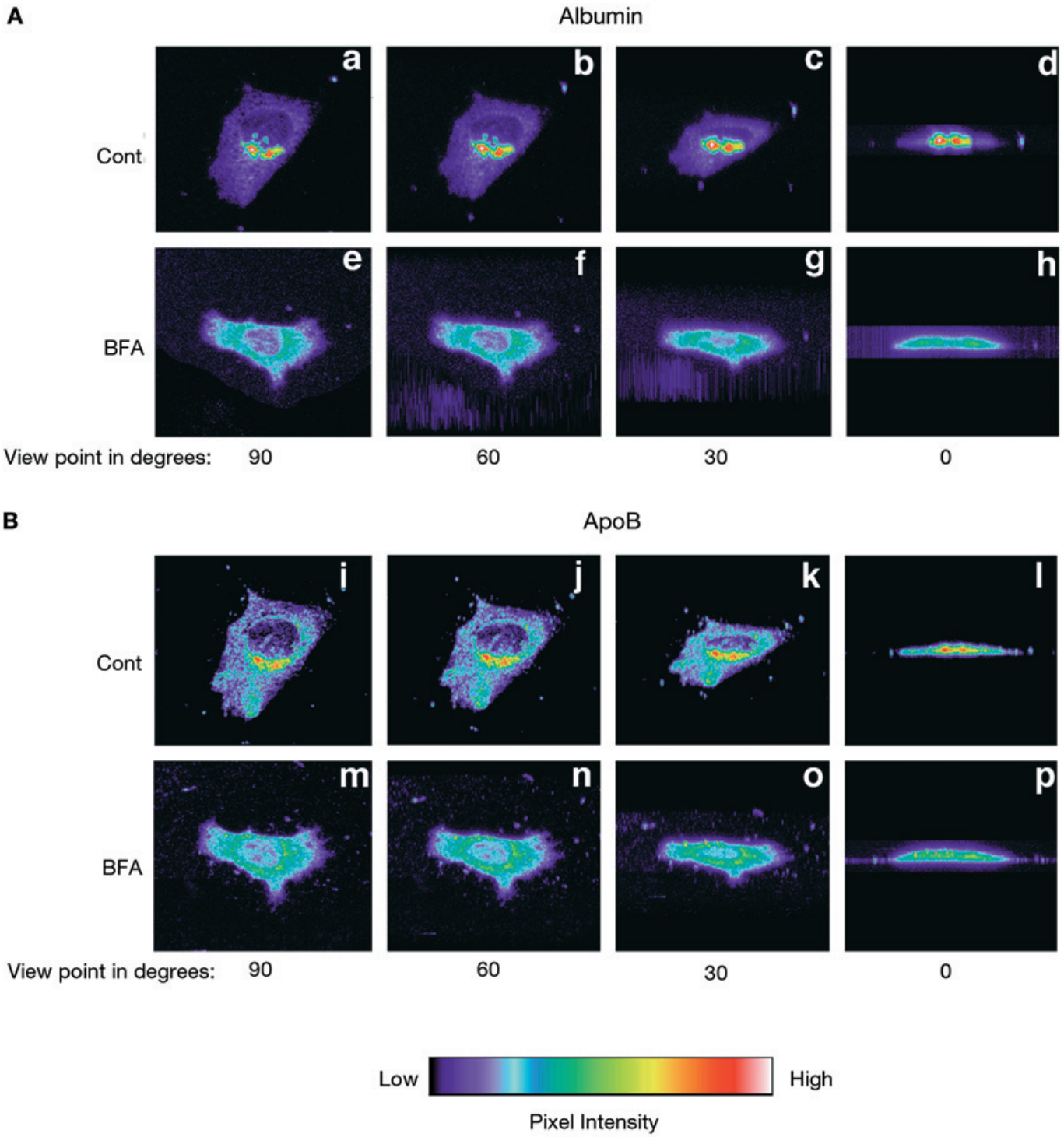

Fig. 4. Three-dimensional distribution of apoB in control and brefeldin-A-treated cells. Three-dimensional constructed images show albumin (A) and apoB (B) distribution in control and brefeldin A-treated cells. Experimental protocol: after preincubation with serum-free medium, HepG2 cells were treated with puromycin to deplete apoB and albumin and then treated in the absence (Cont) or presence of brefeldin A (BFA) as described in Fig. 3. After 60 min of reinitiation with or without brefeldin A, cells were fixed, permeabilized, and probed with (A) anti-albumin (1:2,500 dilution; a–h) and (B) anti-apoB (C1.4, 1:100 dilution; i–p) followed by the appropriate secondary antibodies (1:100 final dilution). Multiple horizontal sections of cells were collected, three-dimensional images were constructed, and signal intensity was converted into pseudocolor (see color table of pixel intensity) as described in Materials and Methods. a, e, i, and m: Three-dimensional images from the 90° viewpoint (i.e., from directly above). b, f, j, and n: Images from the 60° viewpoint. c, g, k, and o: Images from the 30° viewpoint. d, h, l, and p: Images from the 0° viewpoint (i.e., from the side).

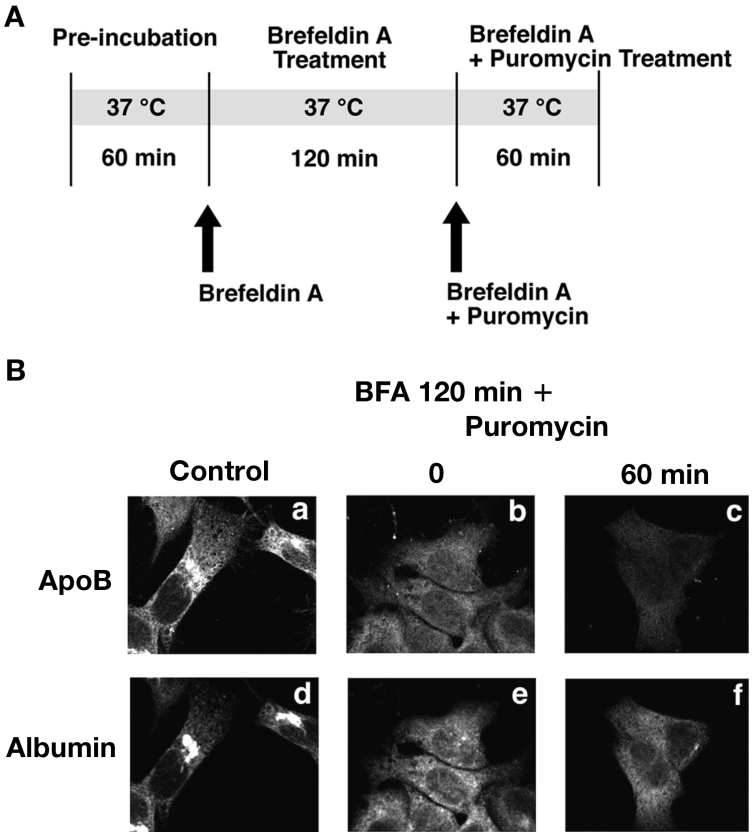

Fig. 5. Distribution of ER-associated proteasomal degradation of apoB. A: Experimental procedure: HepG2 cells were preincubated with serum-free medium for 60 min and then incubated in medium containing brefeldin A (BFA) (2 μg/ml) to inhibit secretory protein transport from the ER to Golgi. After 120 min, cells were incubated for 60 min with brefeldin A in the presence of puromycin (20 μM) to prevent replenishment of apoB and albumin in the ER. At 0 or 60 min, cells were fixed, permeabilized, and probed with anti-apoB (C1.4, 1:100 dilution; a–c) and anti-albumin (1:2,500; d–f). B: Control shows cells before brefeldin A treatment (a and d). b and e: Signals after 120 min of brefeldin A treatment. c and f: Signals after brefeldin A and puromycin treatment.

hibited ER-to-Golgi transport with brefeldin A and then, in order to prevent replenishment of the ER apoB pool, stopped apoB synthesis with puromycin (see protocol, **Fig. 5A**). After 120 min of brefeldin A treatment alone, apoB and albumin were detected in the ER but not in the Golgi (Fig. 5B, panels b and e). As observed in cells with reinitiated protein synthesis (Fig. 3B, panel b), there were no subdomains of the ER or cell with increased apoB signal. Puromycin was then added and after 60 min of incubation at 37°C, apoB signal intensity was observed to have decreased uniformly throughout the ER (Fig. 5B, panel c). In the same cell, the albumin signal was maintained in the ER (Fig. 5B, panel f), indicating that albumin was not degraded (34). Analysis of signal intensities of the entire nonnuclear region of cells (**Fig. 6**) indicated that approximately 60% of the apoB mean pixel intensity was lost after 60 min ($P < 0.001$) whereas the albumin signal was maintained during treatment with puromycin. Similar results, but with smaller changes in apoB signal, were observed after 30 min of puromycin treatment (data not shown).

To map the distribution of apoB when apoB degradation was inhibited in brefeldin A-treated cells, a proteasome inhibitor, *clasto*-lactacystin β-lactone (20 μM), was added to the cells with brefeldin A. Because ER-to-Golgi transport was blocked, the staining represents apoB only in the ER. Without proteasome inhibitor (**Fig. 7**, left), the mean pixel intensity of apoB signal [58.6 ± 5.6 arbitrary units (±SD), n = 5] in the entire ER network was significantly lower ($P < 0.001$) than the intensity [110.0 ± 13.1 arbitrary units (±SD), n = 5] in cells with proteasome inhibitor (Fig. 7, right). The apoB signal in some regions of the ER appeared notably accentuated in *clasto*-lactacystin β-lactone-treated cells, but these regions represented a large percentage of the entire ER and did not appear to constitute a subdomain or a specific organelle. These experiments show that loss of apoB signal occurs widely and homogeneously throughout the ER region in brefeldin A-

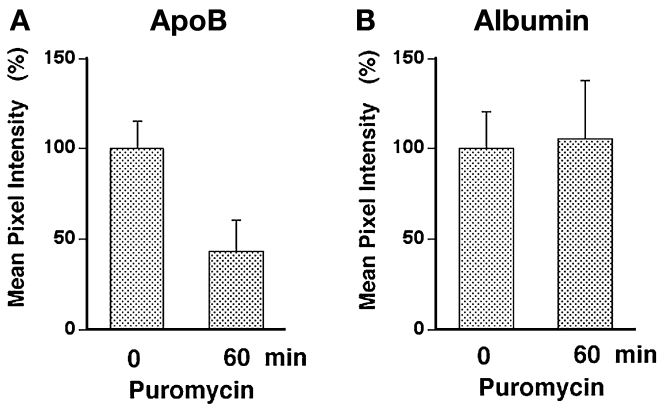

Fig. 6. Comparison of apoB and albumin signals in HepG2 cells. The apoB and albumin signals from the experiment shown in Fig. 5 were analyzed by NIH Image as described in Materials and Methods. A total of 10 cells from two different experiments were analyzed. The mean pixel intensity from 10 cells after 60 min of puromycin treatment was compared with that of 10 cells before puromycin treatment (designated as 100%). A: ApoB; B: albumin. Columns and bars show means ± SD.

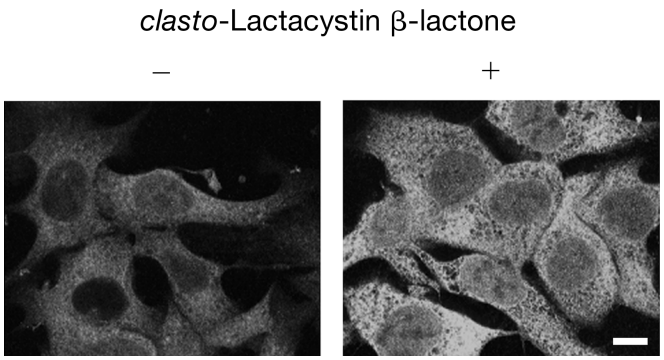

Fig. 7. Distribution of apoB in the ER during inhibition of the proteasome. HepG2 cells were preincubated with serum-free medium for 60 min and then incubated for 2 hr in medium containing brefeldin A (2 μg/ml) to inhibit secretory protein transport from ER to Golgi in the absence (left) or presence (right) of a proteasome inhibitor, *clasto*-lactacystin β-lactone (20 μM). Cells were fixed, permeabilized, and probed with anti-apoB (C1.4). Images were obtained during the same session under identical laser and microscope conditions. Magnification bar: 10 μm.

treated cells and could be prevented when the proteasome was inhibited.

Localization of proteasomes in digitonin-permeabilized cells

We previously showed that two separate epitopes in apoB colocalized with zeta and HC10 subunits of the 20S proteasome (17). Colocalization was confirmed in the current study by probing for the intracellular location of an additional proteasome subunit, LMP7. When digitonin-permeabilized cells with intact ER (**Fig. 8**) were probed simultaneously with an antibody to LMP7 and the CC3.4 antibody to apoB, there was good overlap in the signals throughout the cell, although the signal for LMP7 was smoother and more continuous than the punctate signal for apoB. The CC3.4 antibody was used because it can recognize apoB in digitonin-permeabilized cells, as its epitope is located on the cytosolic side of the ER membrane (22). As washing digitonin-permeabilized cells will cause loss of soluble cytosolic components, the signals for LMP7 probably emanate from proteasomes that are associated with internal membranes, especially those on the cytosolic side of the ER. Immunoelectron microscopy and nanogold labeling were used to probe the location of the proteasome more precisely (**Fig. 9**). Silver-enhanced gold particles were observed in close proximity to the ER membrane when digitonin-permeabilized cells were probed with anti-proteasome subunit HC10. The more highly magnified image in Fig. 9B shows silver-coated gold particles immediately next to the ER membrane or on the ER membrane. These observations provide support for the blueprint suggesting that the machinery of proteasomal degradation is located, in addition to other places in the cell, near or on the cytosolic side of the ER membrane and, like apoB, is distributed throughout the extensive ER network. We hypothesize that the proteasomes that are most likely responsible for rapid degradation of newly synthesized apoB are located throughout the ER region in close proximity to apoB, but on the opposite side (i.e., the cytosolic face) of the ER membrane.

DISCUSSION

In a previous immunocytochemistry study (22), we observed apoB staining throughout the ER but could not distinguish between apoB in ER and Golgi compartments. In the current study, it was possible to monitor apoB transport between ER and Golgi by using the C1.4 monoclonal anti-apoB antibody, which recognizes amino acids 470–526 in apoB (35). This antibody produced stronger signals for apoB in the Golgi than any other antibodies we have used (22), possibly because its epitope in apoB remains unobstructed in lipidated apoB-lipoproteins in the Golgi. The epitope for C1.4 in apoB is located in the lu-

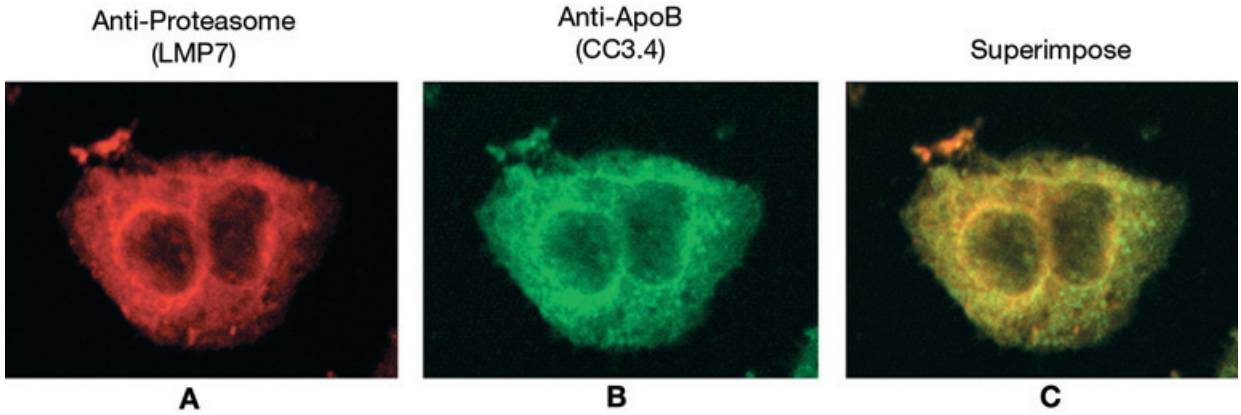

Fig. 8. Proteasome subunit LMP7 and apoB colocalize in the ER of HepG2 cells. Cells were incubated for 1 h in serum-free medium, fixed, permeabilized with digitonin (60 μg/ml) for 5 min at 4°C, and washed before processing for immunocytochemistry. Permeabilized cells were probed simultaneously with rabbit anti-proteasome subunit LMP7 (A, 1:100 final dilution) and mouse anti-apoB antibody CC3.4 (B, 1:200 dilution) followed by anti-mouse and anti-rabbit IgG secondary antibodies (1:100 dilution) conjugated with fluorochromes (Cy3 or Cy5). C: A superimposed picture of (A) and (B); colocalization of LMP7 and apoB is shown as yellow.

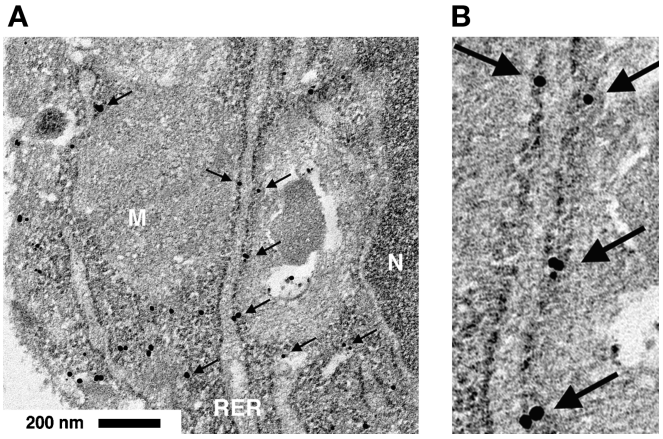

Fig. 9. Proteasome is associated with the ER membrane in HepG2 cells. HepG2 cells were fixed with 2% paraformaldehyde and permeabilized with digitonin (60 μg/ml) as described in Materials and Methods. The cells were incubated with anti-proteasome HC10 subunit antibody followed by secondary antibody conjugated with nanogold particles. After washing, cells were processed to observe proteasome-bound nanogold under an electron microscope. A: Arrows point to nanogold particles enlarged by silver coating. N, M, and RER denote nucleus, mitochondrion, and rough endoplasmic reticulum, respectively. B: Enlarged (2.4×) micrograph of (A).

men of the secretory pathway as saponin permeabilization is required to detect it (data not shown).

Keller et al. (36) previously studied albumin and apoB synthesis and transport in the secretory pathway of rat hepatocytes, using cycloheximide to synchronize protein synthesis. In their study, the sites of apoB and albumin synthesis and their distribution in the ER did not colocalize at early time points, probably the result of lower sensitivity of the epifluorescence methods used and the inability to block the rapid transport of albumin from ER to Golgi. By using puromycin, brefeldin A, and confocal microscopy, the current immunocytochemical study visualized albumin and apoB distribution in the ER in greater detail and with the ability to interrupt transport between compartments.

ApoB distribution and transport in the unblocked secretory pathway

When ER-to-Golgi transport was normal, both apoB (Fig. 4B, panels i–l) and albumin (Fig. 4A, panels a–d) were distributed throughout the entire ER network and in the Golgi 60 min after reinitiation of protein synthesis. Analysis of the signal distributions of albumin and apoB in Fig. 4 indicated that approximately 50% of the albumin signal was found in the Golgi compared with only 10% for apoB (data not shown). The high concentration of albumin in Golgi supports observations that albumin travels from ER to Golgi faster than most other secretory proteins (37). Interestingly, the Golgi spanned almost the entire thickness in HepG2 cells, leaving open the possibility that Golgi-to-plasma membrane transport is vectorally directed to where the Golgi comes closest to the plasma membrane.

Although our studies show good overlap of apoB and albumin in Golgi, the resolution is only that allowed by light microscopy. A previous immunogold electron microscopy study of rat liver showed that albumin and apoB are not completely colocalized in Golgi (38). Whereas albumin was uniformly distributed throughout the Golgi stacks, apoB and apoE were restricted to peripheral enlarged saccular distensions of about 250 nm in diameter, suggesting that enlarged VLDL particles require a larger lumen volume in the Golgi.

ApoB distribution in brefeldin A-blocked cells

When ER-to-Golgi transport was prevented by collapsing the Golgi with brefeldin A (39), both apoB and albumin accumulated in the ER. Closer inspection of the three-dimensional images of transport blocked cells indicated that there was a ribbon of more intense signal for both proteins in the central portion of the ER. It is not known whether this build-up represents increased synthesis in these areas or increased congregation during intra-ER transport. The movements of soluble and membrane proteins within and between cell compartments of the secretory pathway are extremely rapid, occurring within minutes if not seconds (40–42).

It is not known whether apoB is constrained in the ER membrane or whether it is completely diffusible like other ER membrane or lumenal proteins. The most crucial observation from three-dimensional analysis of apoB and albumin distribution in normal cells and in cells with blocked ER-to-Golgi transport is that these two proteins, with vastly different posttranslational processing requirements, are both distributed similarly throughout the ER network and in the Golgi. This is the first study that can visually distinguish between apoB in the ER and apoB in the Golgi compartments and allows comparison of its distribution with that of albumin.

Effect of MTP inhibitor on apoB ER-to-Golgi transport

Whereas ER-to-Golgi transport of both apoB and albumin was inhibited by brefeldin A, only apoB transport was greatly affected by CP-10447, an inhibitor of MTP. Inhibition of MTP prevents the early transfer of triglyceride and phospholipid to apoB in the ER (43). We interpret the experiment in Fig. 3, showing that apoB remains in the ER in CP-10447-treated cells, as indicating that inhibition of MTP prevents apoB from being made into a nascent lipoprotein and packaged into transport vesicles, possibly because of improper nascent apoB lipoprotein particle size or abnormal protein conformation. The exact role of MTP in apoB-lipoprotein assembly is still under investigation. Inhibition of MTP slows apoB translocation across the ER membrane and conversion to a nascent apoB particle (10). CP-10447 was also shown to slow apoB synthesis, possibly through feedback from the stress response to unfolded proteins (44). These studies show that the translation, translocation, and secretion of apoB constitute a delicately balanced system (44). In mouse hepatocytes without MTP expression, Raabe et al. (45) could not observe VLDL-sized, lipid-staining particles in ER or Golgi. Fur-

thermore, there was only a modest decrease in the secretion of apoB-48 in MTP delta/delta mouse hepatocytes, indicating that apoB-48, unlike apoB-100, does not require MTP for transport between ER and Golgi. Studies to date indicate that MTP is important for the formation of a nascent apoB-lipoprotein particle in the ER. Our studies show that the transport of apoB between ER and Golgi is compromised when MTP is inhibited, and suggest that if a lipoprotein particle is not formed, apoB-100 cannot be transported to the Golgi apparatus. This is consistent with the model that MTP inhibition or low lipid availability causes apoB to remain engaged to the ribosome and translocon (25).

Intracellular degradation of nascent apoB

Intracellular degradation of newly synthesized apoB has been observed in hepatoma cells and in primary hepatocytes (2, 46) and is a major regulatory mechanism for apoB secretion (2, 3). Even in the presence of fatty acid, apoB degradation was extremely rapid in HepG2 cells when ER-to-Golgi transport was blocked with brefeldin A (33). Inhibition of the secretory pathway with brefeldin A would favor degradation of apoB in the ER, which in intact HepG2 cells likely involves the proteasome (14–17, 47, 48) and requires cytosolic components (17). Deglycosylation, delipidation and retrograde transport of apoB through the ER membrane would need to occur before degradation by proteasomes in the cytosol or on the cytosolic surface of the ER membrane (17, 23). Even so, degradation of apoB is extremely rapid and efficient as partially degraded intermediates of apoB are difficult to detect, even in lipid-poor HepG2 cells (33). In the current studies, apoB degradation was allowed to occur in live cells and then visualized by immunocytochemistry. Degradation of apoB in the ER may also occur by a nonproteasomal pathway as observed in permeabilized cells with disrupted proteasomal degradation (49). In the ER, apoB was shown to be associated with ER-60, an ER-resident cysteine protease (50).

Location of ER apoB degradation

In the current experiments, an intense build-up of apoB signal was not observed in any ER subdomain or other cell organelle at either 30 min (data not shown), 60 min (Fig. 3B, panel b), or 120 min (Fig. 5B, panel b) in brefeldin A-blocked cells, or in brefeldin A-blocked cells treated with a proteasome inhibitor (Fig. 7). The current data, and the observations that a small portion of the C terminus of apoB remains untranslated until nascent lipoprotein formation (25), suggest a near neighbor proteasome degradation model (**Fig. 10**). Once targeted for degradation, apoB is degraded by a proteasome located in close proximity to the translocon used by an apoB molecule during its synthesis. Incompletely translated apoB may diffuse throughout the ER but would remain linked to the original translocon complex (25). If lipidation and nascent particle formation do not progress sufficiently, apoB is drawn back through the translocon for degradation by a neighboring proteasome. Cytosolic factors (17), including heat shock protein 70 (26), are required for retrotransport and degradation. An alternative model is that apoB is completely translated and translocated, and disengages from the translocon and diffuses throughout the ER before targeting to secretion or retrograde transport (51). Studies of the orientation of apoB in the ER membrane do not support an efficient and complete translocation of apoB before it is targeted for rapid secretion or rapid degradation (52).

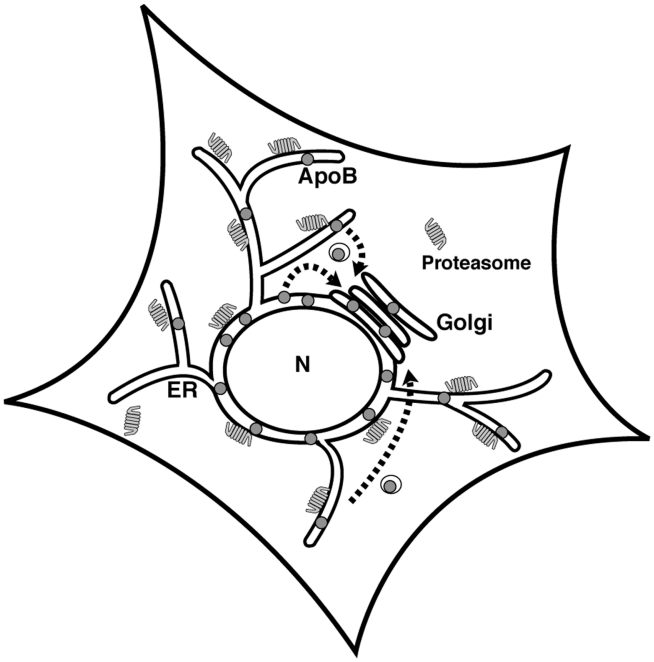

Fig. 10. Model: ApoB is degraded by neighboring proteasomes. ApoB is synthesized throughout the extensive ER network and is transported to the juxtanuclear Golgi. If apoB transport from the ER to the Golgi is blocked (either with brefeldin A or CP-10447), apoB is targeted and then degraded by ER-associated proteasomes on the cytosolic side of the ER membrane. ApoB, which is incompletely translated and translocated (25), undergoes reverse transport through the translocon and is degraded by an available proteasome.

The current observations do not match a model in which apoB is transported to a specific location or organelle for proteasomal degradation, as was shown for excess cystic fibrosis transmembrane conductance regulator polypeptides that become sequestered in the ubiquitin-proteasome enriched centrosome after prolonged treatment with a proteasome inhibitor (53, 54).

Our observations that *1*) ER-associated proteasomal degradation of apoB occurs homogeneously throughout the extensive ER region and does not appear to occur in specific regions of the ER; *2*) apoB accumulates throughout the ER in cells treated with proteasome inhibitors, and *3*) ER-associated proteasomes are also located homogeneously throughout the ER and colocalize with apoB (Fig. 8), are consistent with the near neighbor proteasome degradation model depicted in Fig. 10.

This work was supported by grant HL-47586 to Joseph L. Dixon from the National Heart, Lung, and Blood Institute, National Institutes of Health. An MTP inhibitor, CP-10447, was provided

by Pfizer (Groton, CT). We thank J. Daniel Stoops for excellent technical assistance.

Manuscript received 21 June 2001 and in revised form 27 August, 2001.

REFERENCES

1. Steinberg, D., T. E. Carew, C. Fielding, A. M. Fogelman, R. W. Mahley, A. D. Sniderman, and D. B. Zilversmit. 1989. Lipoproteins and the pathogenesis of atherosclerosis. *Circulation.* **80:** 719–723.
2. Davis, R. A. 1999. Cell and molecular biology of the assembly and secretion of apolipoprotein B-containing lipoproteins by the liver. *Biochim. Biophys. Acta.* **1440:** 1–31.
3. Dixon, J. L., and H. N. Ginsberg. 1993. Regulation of hepatic secretion of apolipoprotein B-containing lipoproteins—information obtained from cultured liver cells. *J. Lipid Res.* **34:** 167–179.
4. Watts, G. F., P. Moroz, and P. H. Barrett. 2000. Kinetics of very-low-density lipoprotein apolipoprotein B-100 in normolipidemic subjects: pooled analysis of stable-isotope studies. *Metabolism.* **49:** 1204–1210.
5. Ginsberg, H. N. 1991. Lipoprotein physiology in nondiabetic and diabetic states. Relationship to atherogenesis. *Diabetes Care.* **14:** 839–855.
6. Alexander, C. A., R. L. Hamilton, and R. J. Havel. 1976. Subcellular localization of B apoprotein of plasma lipoproteins in rat liver. *J. Cell Biol.* **69:** 241–263.
7. Swift, L. L., K. Valyi-Nagy, C. Rowland, and C. Harris. 2001. Assembly of very low density lipoproteins in mouse liver: evidence of heterogeneity of particle density in the Golgi apparatus. *J. Lipid Res.* **42:** 218–224.
8. Wetterau, J. R., L. P. Aggerbeck, M. E. Bouma, C. Eisenberg, A. Munck, M. Hermier, J. Schmitz, G. Gay, D. J. Rader, and R. E. Gregg. 1992. Absence of microsomal triglyceride transfer protein in individuals with abetalipoproteinemia. *Science.* **258:** 999–1001.
9. Jamil, H., J. K. Dickson, Jr., C. H. Chu, M. W. Lago, J. K. Rinehart, S. A. Biller, R. E. Gregg, and J. R. Wetterau. 1995. Microsomal triglyceride transfer protein. Specificity of lipid binding and transport. *J. Biol. Chem.* **270:** 6549–6554.
10. Rustaeus, S., P. Stillemark, K. Lindberg, D. Gordon, and S-O. Olofsson. 1998. The microsomal triglyceride transfer protein catalyzes the post-translational assembly of apolipoprotein B-100 very low density lipoprotein in McA-RH7777 cells. *J. Biol. Chem.* **273:** 5196–5203.
11. Thrift, R. N., J. Drisko, S. Dueland, J. D. Trawick, and R. A. Davis. 1992. Translocation of apolipoprotein B across the endoplasmic reticulum is blocked in a nonhepatic cell line. *Proc. Natl. Acad. Sci. USA.* **89:** 9161–9165.
12. Sakata, N., X. Wu, J. L. Dixon, and H. N. Ginsberg. 1993. Proteolysis and lipid-facilitated translocation are distinct but competitive processes that regulate secretion of apolipoprotein B in Hep G2 cells. *J. Biol. Chem.* **268:** 22967–22970.
13. Bonnardel, J. A., and R. A. Davis. 1995. In HepG2 cells, translocation, not degradation, determines the fate of the de novo synthesized apolipoprotein B. *J. Biol. Chem.* **270:** 28892–28896.
14. Yeung, S. J., S. H. Chen, and L. Chan. 1996. Ubiquitin-proteasome pathway mediates intracellular degradation of apolipoprotein B. *Biochemistry.* **35:** 13843–13848.
15. Fisher, E. A., M. Zhou, D. M. Mitchell, X. Wu, S. Omura, H. Wang, A. L. Goldberg, and H. N. Ginsberg. 1997. The degradation of apolipoprotein B100 is mediated by the ubiquitin-proteasome pathway and involves heat shock protein 70. *J. Biol. Chem.* **272:** 20427–20434.
16. Benoist, F., and T. Grand-Perret. 1997. Co-translational degradation of apolipoprotein B100 by the proteasome is prevented by microsomal triglyceride transfer protein. Synchronized translation studies on HepG2 cells treated with an inhibitor of microsomal triglyceride transfer protein. *J. Biol. Chem.* **272:** 20435–20442.
17. Sakata, N., J. D. Stoops, and J. L. Dixon. 1999. Cytosolic components are required for proteasome degradation of newly synthesized apolipoprotein B in permeabilized HepG2 cells. *J. Biol. Chem.* **274:** 17068–17074.
18. Werner, E. D., J. L. Brodsky, and A. A. McCracken. 1996. Proteasome-dependent endoplasmic reticulum-associated protein degradation: an unconventional route to a familiar fate. *Proc. Natl. Acad. Sci. USA.* **93:** 13797–13801.
19. Wiertz, E. J., D. Tortorella, M. Bogyo, J. Yu, W. Mothes, T. R. Jones, T. A. Rapoport, and H. L. Ploegh. 1996. Sec61-mediated transfer of a membrane protein from the endoplasmic reticulum to the proteasome for destruction. *Nature.* **384:** 432–438.
20. Sommer, T., and D. H. Wolf. 1997. Endoplasmic reticulum degradation: reverse protein flow of no return. *FASEB J.* **11:** 1227–1233.
21. Pilon, M., R. Schekman, and K. Römisch. 1997. Sec61p mediates export of a misfolded secretory protein from the endoplasmic reticulum to the cytosol for degradation. *EMBO J.* **16:** 4540–4548.
22. Du, X., J. D. Stoops, J. Mertz, C. M. Stanley, and J. L. Dixon. 1998. Identification of two regions in apolipoprotein B100 that are exposed on the cytosolic side of the endoplasmic reticulum membrane. *J. Cell Biol.* **141:** 585–599.
23. Zhou, M., E. A. Fisher, and H. N. Ginsberg. 1998. Regulated cotranslational ubiquitination of apolipoprotein B100. A new paradigm for proteasomal degradation of a secretory protein. *J. Biol. Chem.* **273:** 24649–24653.
24. Rusiñol, A. E., R. S. Hegde, S. L. Chuck, V. R. Lingappa, and J. E. Vance. 1998. Translocational pausing of apolipoprotein B can be regulated by membrane lipid composition. *J. Lipid Res.* **39:** 1287–1294.
25. Pariyarath, R., H. Wang, J. D. Aitchison, H. N. Ginsberg, W. J. Welch, A. E. Johnson, and E. A. Fisher. 2001. Co-translational interactions of apoprotein B with the ribosome and translocon during lipoprotein assembly or targeting to the proteasome. *J. Biol. Chem.* **276:** 541–550.
26. Zhou, M., X. Wu, L-S. Huang, and H. N. Ginsberg. 1995. Apoprotein B100, an inefficiently translocated secretory protein, is bound to the cytosolic chaperone, heat shock protein 70. *J. Biol. Chem.* **270:** 25220–25224.
27. Wang, H., X. Chen, and E. A. Fisher. 1993. N-3 fatty acids stimulate intracellular degradation of apoprotein-B in rat hepatocytes. *J. Clin. Invest.* **91:** 1380–1389.
28. Wang, C. N., T. C. Hobman, and D. N. Brindley. 1995. Degradation of apolipoprotein B in cultured rat hepatocytes occurs in a post-endoplasmic reticulum compartment. *J. Biol. Chem.* **270:** 24924–24931.
29. Sparks, J. D., T. L. Phung, M. Bolognino, and C. E. Sparks. 1996. Insulin-mediated inhibition of apolipoprotein B secretion requires an intracellular trafficking event and phosphatidylinositol 3-kinase activation: studies with brefeldin A and wortmannin in primary cultures of rat hepatocytes. *Biochem. J.* **313:** 567–574.
30. Twisk, J., D. L. Gillian-Daniel, A. Tebon, L. Wang, P. H. R. Barrett, and A. D. Attie. 2000. The role of the LDL receptor in apolipoprotein B secretion. *J. Clin. Invest.* **105:** 521–532.
31. Haghpassand, M., D. Wilder, and J. B. Moberly. 1996. Inhibition of apolipoprotein B and triglyceride secretion in human hepatoma cells (HepG2). *J. Lipid Res.* **37:** 1468–1480.
32. Mizuno, M., and S. J. Singer. 1993. A soluble secretory protein is first concentrated in the endoplasmic reticulum before transfer to the Golgi apparatus. *Proc. Natl. Acad. Sci. USA.* **90:** 5732–5736.
33. Furukawa, S., N. Sakata, H. N. Ginsberg, and J. L. Dixon. 1992. Studies of the sites of intracellular degradation of apolipoprotein-B in Hep G2 cells. *J. Biol. Chem.* **267:** 22630–22638.
34. Dixon, J. L., S. Furukawa, and H. N. Ginsberg. 1991. Oleate stimulates secretion of apolipoprotein B-containing lipoproteins from Hep G2 cells by inhibiting early intracellular degradation of apolipoprotein B. *J. Biol. Chem.* **266:** 5080–5086.
35. Krul, E. S., Y. Kleinman, M. Kinoshita, B. Pfleger, K. Oida, A. Law, J. Scott, R. Pease, and G. Schonfeld. 1988. Regional specificities of monoclonal anti-human apolipoprotein B antibodies. *J. Lipid Res.* **29:** 937–947.
36. Keller, G. A., C. Glass, D. Louvard, D. Steinberg, and S. J. Singer. 1986. Synchronized synthesis and intracellular transport of serum albumin and apolipoprotein B in cultured rat hepatocytes as studied by double immunofluorescence. *J. Histochem. Cytochem.* **34:** 1223–1230.
37. Lodish, H. F., N. Kong, M. Snider, and G. J. A. M. Strous. 1983. Hepatoma secretory proteins migrate from rough endoplasmic reticulum to Golgi at characteristic rates. *J. Biol. Chem.* **304:** 80–83.
38. Dahan, S., J. P. Ahluwalia, L. Wong, B. I. Posner, and J. J. M. Bergeron. 1994. Concentration of intracellular hepatic apolipoprotein E in Golgi apparatus saccular distensions and endosomes. *J. Cell Biol.* **127:** 1859–1869.
39. Lippincott-Schwartz, J., L. C. Yuan, J. S. Bonifacino, and R. D. Klausner. 1989. Rapid redistribution of Golgi proteins into the ER in cells treated with brefeldin A: evidence for membrane cycling from Golgi to ER. *Cell.* **56:** 801–813.

40. Presley, J. F., N. B. Cole, T. A. Schroer, K. Hirschberg, K. J. M. Zaal, and J. Lippincott-Schwartz. 1997. ER-to-Golgi transport visualized in living cells. *Nature.* **389:** 81–85.
41. Dayel, M. J., E. F. Y. Hom, and A. S. Verkman. 1999. Diffusion of green fluorescent protein in the aqueous-phase lumen of endoplasmic reticulum. *Biophys. J.* **76:** 2843–2851.
42. Scales, S. J., R. Pepperkok, and T. E. Kreis. 1997. Visualization of ER-to-Golgi transport in living cells reveals a sequential mode of action for COPII and COPI. *Cell.* **90:** 1137–1148.
43. Gordon, D. A. 1997. Recent advances in elucidating the role of the microsomal triglyceride transfer protein in apolipoprotein B lipoprotein assembly. *Curr. Opin. Lipidol.* **8:** 131–137.
44. Pan, M., J-S. Liang, E. A. Fisher, and H. N. Ginsberg. 2000. Inhibition of translocation of nascent apolipoprotein B across the endoplasmic reticulum membrane is associated with selective inhibition of the synthesis of apolipoprotein B. *J. Biol. Chem.* **275:** 27399–27405.
45. Raabe, M., M. M. Veniant, M. A. Sullivan, C. H. Zlot, J. Bjorkegren, L. B. Nielsen, J. S. Wong, R. L. Hamilton, and S. G. Young. 1999. Analysis of the role of microsomal triglyceride transfer protein in the liver of tissue-specific knockout mice. *J. Clin. Invest.* **103:** 1287–1298.
46. Taghibiglou, C., D. Rudy, S. C. Van Iderstine, A. Aiton, D. Covallo, R. Cheung, and K. Adeli. 2000. Intracellular mechanisms regulating apoB-containing lipoprotein assembly and secretion in primary hamster hepatocytes. *J. Lipid Res.* **41:** 499–513.
47. Chen, Y., F. Le Cahévec, and S. L. Chuck. 1998. Calnexin and other factors that alter translocation affect the rapid binding of ubiquitin to apoB in the Sec61 complex. *J. Biol. Chem.* **273:** 11887–11894.
48. Sakata, N., and J. L. Dixon. 1999. Ubiquitin-proteasome-dependent degradation of apolipoprotein B100 in vitro. *Biochim. Biophys. Acta.* **1437:** 71–79.
49. Cavallo, D., D. Rudy, A. Mohammadi, J. Macri, and K. Adeli. 1999. Studies on degradative mechanisms mediating post-translational fragmentation of apolipoprotein B and the generation of the 70-kDa fragment. *J. Biol. Chem.* **274:** 23135–23143.
50. Adeli, K., J. Macri, A. Mohammadi, M. Kito, R. Urade, and D. Cavallo. 1997. Apolipoprotein B is intracellularly associated with an ER-60 protease homologue in HepG2 cells. *J. Biol. Chem.* **272:** 22489–22494.
51. Shelness, G. S., M. F. Ingram, X. F. Huang, and J. A. DeLozier. 1999. Apolipoprotein B in the rough endoplasmic reticulum: translation, translocation and the initiation of lipoprotein assembly. *J. Nutr.* **129:** 456S–462S.
52. Liang, J-S., X. Wu, E. A. Fisher, and H. N. Ginsberg. 2000. The amino-terminal domain of apolipoprotein B does not undergo retrograde translocation from the endoplasmic reticulum to the cytosol. Proteasomal degradation of nascent apolipoprotein B begins at the carboxyl terminus of the protein, while apolipoprotein B is still in its original translocon. *J. Biol. Chem.* **275:** 32003–32010.
53. Wigley, W. C., R. P. Fabunmi, M. G. Lee, C. R. Marino, S. Muallem, G. N. DeMartino, and P. J. Thomas. 1999. Dynamic association of proteasomal machinery with the centrosome. *J. Cell Biol.* **145:** 481–490.
54. Johnston, J. A., C. L. Ward, and R. R. Kopito. 1998. Aggresomes: a cellular response to misfolded proteins. *J. Cell Biol.* **143:** 1883–1898.